

Advanced Microwave Radiometry: Refining Sun-Tracking Technique for Atmospheric Attenuation Retrieval and Sun Brightness Temperature Estimation

Giovanni Stazi¹, Marianna Biscarini¹, Luca Milani², George Brost³

¹ DIET, Sapienza University of Rome, Italy, giovanni.stazi@uniroma1.it, marianna.biscarini@uniroma1.it

² LSE Space GmbH, European Space Agency (ESA-ESOC), Darmstadt, Germany, luca.milani@esa.int

³ Air Force Research Laboratory, Rome, NY, USA, george.brost@us.af.mil

Abstract—Sun-Tracking (ST) is a novel ground-based microwave radiometric technique that allows the retrieval of the slant-path atmospheric attenuation in all-weather conditions as well as the estimation of the Sun brightness temperature. This work proposes a refinement procedure of the ST technique based on taking into account the Sun’s angular size variability throughout the year. We have obtained a reduction up to more than 50% of the standard deviation of the estimated Sun’s brightness temperature. On the other hand, we have demonstrated that the approximation of a constant value for the Sun’s angular size, that strongly limits the precision of the Sun brightness temperature estimation, is acceptable for the ST-based attenuation retrieval algorithm. The study is performed exploiting a three-years dataset of ST measurements collected in Rome NY between 2015 and 2018 at 23.8 (K-band), 31.4 (Ka-band), 72.5 (V-band), and 82.5 (W-band) GHz.

Index Terms—Sun-Tracking microwave radiometry, W-band, slant path attenuation, Sun brightness temperature.

I. INTRODUCTION

The increasing interest of satellite communication systems in millimeter wavelengths frequencies (i.e., from *Ka*-band up to *W*-band) is making the atmospheric channel description at these frequencies a crucial aspect of such applications [1]. Indeed, at these frequencies, the electromagnetic signal degradation is due not only to the rain events but also to the contribution of atmospheric gases that becomes not negligible when the link frequency increases [2], [3]. The few available measurements, due to the lack of dedicated space missions working at such high frequencies, limit both the possibility of developing atmospheric models and the design of satellite missions at millimeter wavelengths [4], [5]. As concerning ground-based measurements, classical radiometers turn out to be unreliable under rainy conditions due to the difficulties in modeling the atmospheric mean radiative temperature (whose characterization is well-known only in clear-sky) [6]. In this context, Sun-tracking (ST) microwave radiometers are powerful instruments able to correctly detect both brightness temperature and atmospheric slant-path attenuation in all-weather conditions. ST is a ground-based radiometric technique ancillary conceived in radioastronomy for the estimation of brightness temperature up to millimeter wavelengths [7] - [9] and recently applied in radiopropagation

for the retrieval of atmospheric slant-path attenuation [10], [11]. It consists in exploiting the Sun as a beacon signal performing measurements by continuously switching the azimuth pointing of the antenna from toward the Sun to off the Sun while changing the elevation to track the Sun during its motion. In this way the radiometer alternately measures the atmospheric noise with and without the contribution of the Sun, thus allowing the inference of information about the atmospheric channel exploiting the difference between two consecutive measurements provided an estimation of the beam-filling factor (i.e., the ratio between the Sun radiation-pattern solid angle and the antenna beamwidth radiation-pattern solid angle) [12].

To date, only few sites in the world are equipped with ST radiometers: Rome (NY, USA) [10], Milan (IT) [13], and Xi’an (CN) [14]. In this work we exploit a three-years dataset of ST measurements collected in Rome NY between 2015 and 2018 at 23.8 (*K*-band), 31.4 (*Ka*-band), 72.5 (*V*-band), and 82.5 (*W*-band) GHz. This unique and large dataset made possible to refine the atmospheric attenuation retrieval technique as well as the precision of the Sun brightness temperature estimation. Indeed, previous works were based on the simplified assumption of a constant value of the beam-filling factor that prevented a reliable estimation of Sun brightness temperature [15]. In this work we propose an update of the ST technique through the introduction of a variable beam-filling factor that takes into account the dependence of the Sun’s angular size on the Earth-Sun distance. This allows a refinement of both the attenuation retrieval algorithm and of the estimated brightness temperature of the Sun.

This work is organized in the following way: in section II the basic theory of ST is reviewed. In section III the measurement instrument and the available dataset are shortly described. In section IV the main results regarding the evaluation of the Sun brightness temperature and the assessment of the retrieved attenuation are presented. Finally, in section V, conclusions are drawn and future developments are discussed.

II. SUN TRACKING TECHNIQUE

This section recalls the basic principles of the ST technique and describes the proposed approach for refining the brightness temperature estimation.

A. *Evaluation of the Sun brightness temperature and of the atmospheric attenuation*

Sun Tracking (ST) is a ground-based microwave radiometric technique consisting in using the Sun as a signal source in order to infer information about the atmosphere. The measurement procedure consists of two consecutive data acquisitions: the first one is performed pointing the radiometer antenna *toward the Sun* (twS) and the second one changing only the azimuth angle of the radiometer's antenna to make it pointing *out of the Sun* (ooS). In the meanwhile, the Sun moves along its diurnal ecliptic and the radiometer follows its movement. By exploiting the difference between the twS and ooS measurements, it is possible to evaluate both the Sun brightness temperature and the path attenuation in all-weather conditions.

ST-MWRs functioning, thoroughly described in [6] and [15], is recalled in the following. When the radiometer points ooS, with an elevation angle θ and an azimuth angle φ_1 , the brightness temperature impinging on the radiometer's antenna is given by the contribution of the sky brightness temperature and of the cosmic background brightness temperature, both attenuated by the atmosphere along the path:

$$T_{B_{ooS}}(\theta, \varphi_1) = T_{mr}(\theta, \varphi_1)[1 - e^{-\tau(\theta, \varphi_1)}] + T_{cos}e^{-\tau(\theta, \varphi_1)} \quad (1)$$

where T_{mr} is the sky mean radiative temperature, τ is the optical thickness along the considered direction (θ, φ_1) , and T_{cos} is the cosmic background brightness temperature (2.73 K). When the radiometer points twS (with the same elevation angle θ and a shifted azimuth angle φ_0), also the Sun brightness temperature $T_{B_{sun}}$, attenuated by the atmosphere, must be considered and the brightness temperature impinging on the radiometer's antenna is then given by

$$T_{B_{twS}}(\theta, \varphi_0) = T_{B_{sun}}e^{-\tau(\theta, \varphi_0)} + T_{mr}(\theta, \varphi_0)[1 - e^{-\tau(\theta, \varphi_0)}] + T_{cos}e^{-\tau(\theta, \varphi_0)}. \quad (2)$$

The antenna noise temperature in the generic direction (θ_0, φ_0) can be evaluated according to [3]

$$T_A(\theta_0, \varphi_0) = \frac{\int_{4\pi} T_B(\theta, \varphi) F_n(\theta_0, \varphi_0, \theta, \varphi) d\Omega}{\int_{4\pi} F_n(\theta_0, \varphi_0, \theta, \varphi) d\Omega} \quad (3)$$

where $F_n(\theta_0, \varphi_0, \theta, \varphi)$ is the normalized antenna power radiation pattern, and it results

$$\int_{4\pi} F_n(\theta_0, \varphi_0, \theta, \varphi) d\Omega = \Omega_{P_{ant}} \quad (4)$$

where $\Omega_{P_{ant}}$ is the radiation-pattern solid angle of the antenna. Assuming a constant atmospheric contribution within the main antenna beam it results, for the ooS observation, $T_{A_{ooS}}(\theta_0, \varphi_1) \cong T_{B_{ooS}}(\theta_0, \varphi_1)$. For the twS case, the antenna noise temperature can be evaluated by inserting (2) into (3) which, after some mathematical calculations, results in

$$T_{A_{twS}}(\theta, \varphi_0) \cong f_{\Omega} T_{B_{sun}} e^{-\tau(\theta, \varphi_0)} +$$

$$+ T_{mr}(\theta, \varphi_0)[1 - e^{-\tau(\theta, \varphi_0)}] + T_{cos}e^{-\tau(\theta, \varphi_0)} \quad (5)$$

where f_{Ω} is the so-called *beam-filling factor*, given by the ratio between the Sun radiation-pattern solid angle $\Omega_{P_{sun}}$ and the antenna beamwidth radiation-pattern solid angle $\Omega_{P_{ant}}$:

$$f_{\Omega} = \frac{\Omega_{P_{sun}}}{\Omega_{P_{ant}}}. \quad (6)$$

Note that (5) is written assuming a uniform Sun brightness temperature within the antenna beam. Making the difference between $T_{A_{twS}}$ and $T_{A_{ooS}}$ we obtain

$$\begin{aligned} \Delta T_A(\theta_0, \varphi_0) &= T_{A_{twS}}(\theta, \varphi_0) - T_{A_{ooS}}(\theta_0, \varphi_1) \cong \\ &\cong f_{\Omega}(\theta_0, \varphi_0) T_{B_{sun}} e^{-\tau(\theta_0, \varphi_0)} \end{aligned} \quad (7)$$

where we are assuming that the switch between the two measurements is fast enough and that the azimuth-shift angle is the minimum that allow that, during the ooS measurement, the Sun is just outside the main beam, in order to consider $T_{mr}(\theta, \varphi_0) \cong T_{mr}(\theta, \varphi_1)$ and $\tau(\theta, \varphi_0) \cong \tau(\theta, \varphi_1)$. The product of the beam-filling factor and the brightness temperature of the Sun is usually referred to as

$$T_{B_{sun}}^* = f_{\Omega}(\theta_0, \varphi_0) T_{B_{sun}}. \quad (8)$$

Note that, in clear-air conditions, starting from (7) it is possible to estimate the Sun brightness temperature provided the knowledge of the beam-filling factor and an estimate of the atmospheric optical thickness τ :

$$T_{B_{sun}} = \frac{T_{B_{sun}}^*}{f_{\Omega}} = \frac{1}{f_{\Omega}} [\Delta T_A(\theta_0) e^{\tau(\theta_0)}]. \quad (9)$$

In (9), the optical thickness in clear-air can be estimated through the so-called meteorological technique considering that

$$\tau(\theta_0) = \ln \left[\frac{T_{mr}(\theta_0) - T_{cos}}{T_{mr}(\theta_0) - T_{A_{ooS}}(\theta_0)} \right] \quad (11)$$

and assuming, for the T_{mr} , classical clear air models based on surface measurements of pressure, temperature and relative humidity [15]. The beam-filling factor is defined as [15]

$$f_{\Omega} = \eta_{ML} \left[1 - e^{-\ln(2) \left(\frac{\Theta_{sun}}{\Theta_{ML}} \right)^2} \right] \quad (12)$$

where η_{ML} is the antenna main beam efficiency (equal to the ratio between the main lobe radiation solid angle and the antenna one), Θ_{sun} is the angular diameter of the Sun, and Θ_{ML} is the half-power beamwidth of the antenna main beam.

Once $T_{B_{sun}}$ (which is supposed to be a constant value) is known from clear-sky ST measurements, $T_{B_{sun}}^*$ in all-weather can be derived through (8) and it is possible to evaluate the atmospheric attenuation $A_{ST}(\theta_0, \varphi_0)$ along the slant-path (θ_0, φ_0) in all-weather conditions:

$$A_{ST}(\theta_0, \varphi_0) = 4.343 \tau(\theta_0, \varphi_0) = 4.343 \ln \left[\frac{T_{B_{sun}}^*(\theta_0, \varphi_0)}{\Delta T_A(\theta_0, \varphi_0)} \right]$$

(13)

where the attenuation is expressed in dB . Equation (13) shows a dependance of the retrieved attenuation on the antenna noise temperature difference. When the weather is cloudy or rainy the contribution of the Sun to the antenna temperature decreases, thus the antenna noise temperature difference decreases as well, leading to an increase in the atmospheric extinction. In case of a heavy precipitation the contribution of the Sun could become so small that could be considered negligible, in this case the antenna noise temperature difference could reach zero or even negative values. This represents the upper limit of the ST technique for the retrieval of the attenuation.

B. Refinement of the Sun brightness temperature estimation

Previous works based on ST measurements considered a constant value of the beam-filling factor assuming a uniform Sun disk [15]. In this work we have evaluated it by taking into account the dependance of the Sun's angular size Θ_{sun} to the Earth-Sun distance D . The Sun's angular size depends on the distance between the Earth and the Sun according to the following formula [16]:

$$\Theta_{sun} = 2 \arcsin\left(\frac{d_{sun}}{2D}\right) \quad (13)$$

where d_{sun} is the diameter of the Sun, equal to about $13.9140 \cdot 10^8 m$. When the Sun is furthest from the Earth ($D \cong 152.1 \cdot 10^6 km$) the Sun's angular size is minimum and equal to about 0.524° , vice versa when the Sun is nearest to the Earth ($D \cong 147 \cdot 10^6 km$) the Sun's angular size is maximum and equal to about 0.542° . The value of the Sun's angular size affects the beam-filling factor f_Ω according to (12).

III. EXPERIMENTAL SETUP

As previously stated, the data used in this work have been collected in Rome NY, USA, ($43.2^\circ N$, $75.4^\circ W$) between May 2015 and September 2018 [10]. The radiometer, located at the Air Force Research Laboratory (AFRL), is a water-vapor and cloud-liquid oriented model (RPG-LWP-U72-82) that has been modified in order to be capable of following the movement of the Sun along its diurnal ecliptic and to perform switching measurements [11]. It has four channels at 23.8, 31.4, 72.5 and 82.5 GHz: the first two channels are at K -band, and the other two at V -, and W -band. The radiation pattern of the antenna can be considered Gaussian with half-power beamwidths equal to 3.74° , 2.97° , 1.47° , and 1.30° at 23.8, 31.4, 72.5 and 82.5 GHz, respectively. The switching mechanism has a resolution of 0.15° in elevation and 0.1° in azimuth. The radiometer takes input data (latitude, longitude, and time) in order to track the Sun. It performs a twS measurement and, after 6 s, switches the azimuth angle from φ_0 to φ_1 to perform the corresponding ooS measurement. In each case the integration time is set to 1 s so that the integrations are performed with a fixed antenna position [15].

The measurement dataset consists of 994 days from 04/05/2015 to 25/09/2018. After a data quality process, the final dataset is composed by 80% of uncorrupt measurements, 5.9% of originally corrupt but then fixed measurements, 7.3% of data corrupt and unrecoverable and 6.8% of unavailable data.

IV. RESULTS AND DISCUSSION

TABLE I. reports the obtained minimum and maximum values of the beam-filling for the four channels' frequencies for one revolution of the Earth around the Sun (i.e., for one year) using ephemeris data for determining the Sun-Earth distance during the year.

TABLE I.
MINIMUM AND MAXIMUM BEAM-FILLING FACTOR OVER ONE YEAR FOR THE FOUR CHANNELS' FREQUENCIES.

Frequency [GHz]	$f_{\Omega,MIN}$	$f_{\Omega,MAX}$
23.8	0.0131	0.0140
31.4	0.0207	0.0221
72.5	0.0825	0.0880
82.5	0.1043	0.1111

This beam-filling factor timeseries can be used to refine the calculation of the antenna noise temperature difference and, consequently, of the atmospheric attenuation according to (7) and (13), respectively. In addition, the Sun brightness temperature estimation can be performed through (8) exploiting the time-series of both the beam-filling factor and of the T_{BSun}^* obtained from measurements. Since T_{BSun} is supposed to be a constant quantity (at each channel frequency), its value is computed as a mean value of the estimated time-series. TABLE II. reports a comparison, in terms of mean value and standard deviation, of the T_{BSun} obtained using a constant value of the beam-filling factor (in line with previous works) and the one obtained using the beam-filling factor time series computed in this work taking into account the dependance on the Sun's angular size. The table highlights that, using the beam-filling factor time-series, the standard deviation is strongly reduced (of about 35% in V - and W -band, and up to more than 50% in Ka -band), thus confirming a more precise estimation of the T_{BSun} .

Finally, to further improve the accuracy of the retrieved attenuation, we can get a more stable and reliable timeseries of T_{BSun}^* using (8) and exploiting the estimated mean value of T_{BSun} together with the beam-filling factor timeseries. This new time-series of T_{BSun}^* can be used for estimating the atmospheric attenuation with (9) eliminating in this way all the variability and errors that come from the measurement procedures. Note that, in previous works, since the beam filling factor was assumed constant, also T_{BSun}^* was a constant quantity (directly derived from clear-sky measurements as described in Section II).

TABLE II.
MEAN AND STANDARD DEVIATION OF THE BRIGHTNESS TEMPERATURE OF THE SUN FOR THE FOUR FREQUENCIES IN THE CASE A CONSTANT BEAM-

Frequency [GHz]	T_{Bsun} mean, using constant beam-filling factor [K]	T_{Bsun} std, using constant beam-filling factor [K]	T_{Bsun} mean, using variable beam-filling factor [K]	T_{Bsun} std, using variable beam-filling factor [K]
23.8 GHz	8984	198.49	9041	106.63
31.4 GHz	8754	205.73	8813	100.76
72.5 GHz	6710	215.92	6753	138.45
82.5 GHz	6595	200.43	6640	130.96

Fig. 1 shows, for the four channel frequencies, a density scatterplot comparing the atmospheric attenuations obtained using a constant value of the beam-filling factor (y-axis) and using the beam-filling factor time-series (x-axis). The figure highlights that the attenuation in the two cases is very similar. This means that the approximation of a constant beam-filling factor, that strongly limits the precision of the Sun brightness temperature estimation, is acceptable for the attenuation retrieval algorithm.

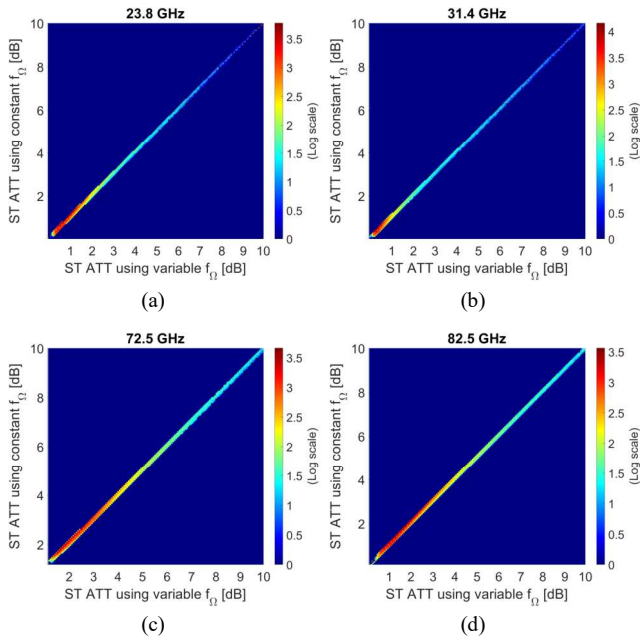


Fig. 1: density scatterplot of the atmospheric attenuation obtained using a constant beam-filling factor versus the one obtained using beam-filling factor time-series at (a) 23.8 GHz, (b) 31.4 GHz, (c) 72.5 GHz, (d) 82.5 GHz.

A further comparison is in Fig. 2 that shows the Complementary Cumulative Distribution Function (CCDF) of the attenuation for the four channel frequencies. The blue curve is obtained using a constant value of the beam-filling factor, the red curve is obtained using the beam-filling factor time-series, the yellow dashed line is obtained following the

recommendation ITU-R 618 from the Radiocommunication Sector of the International Telecommunication Union [17]. The figure confirms the slight and negligible difference between the attenuation computed assuming a constant value of the beam-filling factor and the one computed with the beam-filling factor time-series. The CCDF of the ST-measured attenuation is in good agreement with the one provided by ITU, especially at Ka -band and for low attenuation values (i.e., in clear-sky and in cloudy and light rain conditions).

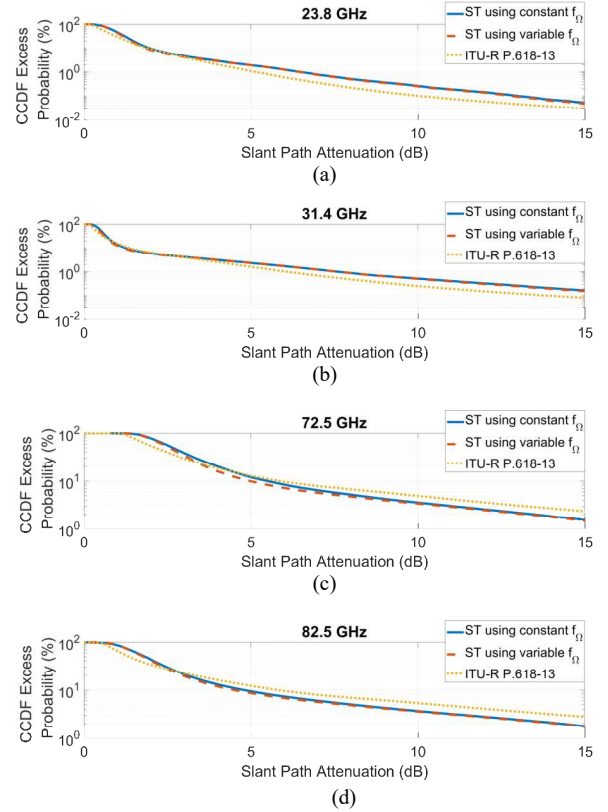


Fig. 2: CCDF of atmospheric attenuation obtained using: constant beam-filling factor (blue), beam-filling factor time-series (red), ITU-R P.618 (yellow dashed) at (a) 23.8 GHz, (b) 31.4 GHz, (c) 72.5 GHz, (d) 82.5 GHz.

V. CONCLUSIONS

This work proposes a refinement procedure of the ST microwave radiometric technique for the assessment of the retrieval of the atmospheric attenuation and the estimation of the Sun brightness temperature. The improvement with respect to previous works based on ST technique is that the Sun's angular size variability throughout the year, which depends on the Earth-Sun distance, was taken into account; this affects both the attenuation retrieval and the evaluation of the Sun's brightness temperature using Sun-Tracking measurements.

We have obtained a reduction up to more than 50% of the standard deviation of the estimated Sun's brightness temperature when considering the Earth-Sun distance variability. On the other hand, we have demonstrated that the approximation of a constant value for the Sun's angular size,

that strongly limits the precision of the Sun brightness temperature estimation, is acceptable for the ST-based attenuation retrieval algorithm.

Future works will be focused on the investigation of the benefits of taking into account the variability of the Sun's angular size in the evaluation of the Sun brightness temperature.

IEEE Journal of Selected Topics in Applied Earth Observations and Remote Sensing, vol. 10, no. 7, pp. 3134–3147, Jul. 2017, doi: 10.1109/JSTARS.2016.2633439.

- [16] W. H. Beyer, "CRC Standard Mathematical Tables," 31st ed., Boca Raton, FL: CRC Press, pp. 342-343, 2003.
- [17] *Propagation Data and Prediction Methods Required for the Design of Earth-Space Telecommunication Systems*, document ITU-R.-P 618-13, Int. Telecommun. Union-Radiopropagation (ITU-R), Dec. 2017.

REFERENCES

- [1] L. J. Ippolito, "Radio propagation for space communications systems," *Proceedings of the IEEE*, vol. 69, pp. 697–727, 1981.
- [2] B. R. Arbesser-Rastburg and A. Paraboni, "European research on Ka-band slant path propagation," *Proceedings of the IEEE*, vol. 85, no. 6, pp. 843–852, Jun. 1997.
- [3] F. T. Ulaby, R. K. Moore, and A. K. Fung, *Microwave Remote Sensing Active and Passive*. Reading, MA, USA: Addison, 1981, vol. 1, pp. 288–302.
- [4] M. Biscarini, M. Montopoli and F. S. Marzano, "Evaluation of High-Frequency Channels for Deep-Space Data Transmission Using Radiometeorological Model Forecast," *IEEE Transactions on Antennas and Propagation*, vol. 65, no. 3, pp. 1311-1320, March 2017 (doi: 10.1109/TAP.2017.2653420).
- [5] D. C. Hogg and T.-S. Chu, "The role of rain in satellite communications," *Proceedings of the IEEE*, vol. 63, no. 9, pp. 1308–1331, Sep. 1975. doi: 10.1109/PROC.1975.9940.
- [6] F. S. Marzano, V. Mattioli, L. Milani, K. M. Magde, and G. A. Brost, "Sun-tracking microwave radiometry: All-weather estimation of atmospheric path attenuation at Ka-, V-, and W-band," *IEEE Transactions on Antennas and Propagation*, vol. 64, no. 11, pp. 4815–4827, Nov. 2016, doi: 10.1109/TAP.2016.2606568.
- [7] R. J. Coates, "Measurements of solar radiation and atmospheric attenuation at 4.3-millimeters wavelength," *Proceedings of the IRE*, vol. 46, pp. 122–126, Jan. 1958.
- [8] F. I. Shimabukuro and J. M. Stacey, "Brightness temperature of the quiet sun at centimeter and millimeter wavelengths," *The Astrophysical Journal*, vol. 152, p. 777, Jun. 1968.
- [9] M. M. Franco, S. D. Slobin, and C. T. Stelzried, "20.7- and 31.4-GHz solar disk temperature measurements," *Jet Propulsion Laboratory*, Pasadena, CA, USA, TDA Progr. Rep. 42-64, 1981, pp. 140–168
- [10] M. Biscarini, G. Stazi, et al., "Statistical Modeling of Atmospheric Propagation Channel at W-Band Through Sun-Tracking Microwave Radiometric Measurements for Non-Geostationary Satellite Links," in *IEEE Transactions on Antennas and Propagation*, vol. 71, no. 9, pp. 7512-7522, Sept. 2023, doi: 10.1109/TAP.2023.3296852.
- [11] G. Brost and K. M. Magde, "On the use of the radiometer formula for atmospheric attenuation measurements at GHz frequencies," in *2016 10th European Conference on Antennas and Propagation (EuCAP)*, Davos, Switzerland, Apr. 2016, pp. 1–5.
- [12] M. Biscarini et al., "Exploiting Tropospheric Measurements From Sun-Tracking Radiometer for Radiopropagation Models at Centimeter and Millimeter Wave," in *IEEE Journal of Selected Topics in Applied Earth Observations and Remote Sensing*, vol. 12, no. 6, pp. 1697-1708, June 2019, doi: 10.1109/JSTARS.2019.2916372.
- [13] F. S. Marzano et al., "Development and Application of Microwave Radiometric Techniques for Modeling Satellite-Earth Propagation at V and W Band," *2021 15th European Conference on Antennas and Propagation (EuCAP)*, Dusseldorf, Germany, 2021, pp. 1-5, doi: 10.23919/EuCAP51087.2021.9410909.
- [14] L. Lei et al., "Measurement of Solar Absolute Brightness Temperature Using a Ground-Based Multichannel Microwave Radiometer," *Remote Sensing*, vol. 13, no. 15, p. 2968, Jul. 2021, doi: 10.3390/rs13152968.
- [15] V. Mattioli, L. Milani, K. M. Magde, G. A. Brost, and F. S. Marzano, "Retrieval of sun brightness temperature and precipitating cloud extinction using ground-based sun-tracking microwave radiometry,"